Acta Physica Universitatis Comenianae
Vol. XLVIII XLIX, Number 1&2 (2007 2008) 71 84

Slovakia in Experiment ATLAS Summary Review

(*submitted to Acta Physica Universitatis Comenianae*)

D. Bruncko[1], P. Šťavina[2], P. Stríženec[1], S. Tokár[2], T. Ženiš[2]

[1]IEP SAS Košice, [2]Comenius University, Bratislava

Abstract: The CERN's new particle accelerator, the Large Hadron Collider, is expected to start up in May 2008. One of the experiments using this accelerator is the experiment ATLAS. The experiment ATLAS is a general purpose experiment on the field of particle physics. The Slovak institutes (Comenius University Bratislava and Institute of Experimental Physics, Slovak Academy of Sciences, Košice) are members of the experiment. Our contribution to this experiment is well accepted within the ATLAS community. Our main obligations are linked to calorimetry especially some tasks concerning the calibration. Besides this we deal with some physics tasks such as top quark physics, as well.

1. Experiment ATLAS

ATLAS (**A T**oroidal **L**HC **A**pparatu**S**) is one of the five particle detector experiments (ALICE, ATLAS, CMS, TOTEM, and LHCb) being constructed at the Large Hadron Collider, a new particle accelerator at CERN in Switzerland. It will be 45 long and 25 meters in diameter, and will weigh about 7,000 tones. The project involves roughly 2,000 scientists and engineers at 151 institutions in 34 countries. The construction is scheduled to be completed in April 2008. The experiment is expected to investigate the phenomena that involve highly massive particles which were not measurable using the earlier accelerators with lower energies and might shed light on new theories of particle physics beyond the Standard Model [1].

The main physics goal of the experiment ATLAS is to explore the Higgs sector of the Standard Model (SM) and alternatively to look for a new physics (physics beyond SM). The other important goal is to overlook the option of the SUSY extension of the Standard Model. Since LHC will be the most powerful top-factory ever built, the top quark physics is therefore natural and very important part of the ATLAS physics programme and can also provide a significant window for possible discoveries beyond the SM.

The experiment ATLAS has approximately cylindrical shape and it consists of a few main parts. The **Inner Tracker** is placed in the center of detector cylinder. Its basic function is to track charged particles by detecting their interaction with material at discrete points, revealing detailed information about the type of particle and its momentum. The next part of the detector is the **Calorimetric System**. The calorimeters are located outside the solenoidal magnet that surrounds the inner detector. Their purpose is to measure the energy from particles by absorbing it. The calorimetric system consists of Liquid Argon calorimeter part (Electromagnetic Barrel EMB, Electromagnetic EndCap EMEC, Hadronic EndCap HEC and Forward calorimeter FW) and central and extended barrel scintillating calorimeter with iron absorber TileCal. The next part of the detector is the

Devoted to Prof. Pavel Povinec 65-th anniversary

Muon Spectrometer. It is intended to measure precisely momenta of muons penetrating through the calorimetric system. Important part of the experiment is its **Magnetic System**. It consists of the inner solenoid and outer toroids. Its purpose is to curve particle trajectory for the particle momentum measurement.

2. Slovak contribution to experiment ATLAS

As it has already been mentioned, our institutes have been participating in the development and testing of the calorimetric system. We have got the strict obligations in frame of construction and development of the TileCal and HEC subsystems (subdetectors). Our main obligation is development of the electronic calibration system for HEC. Within the mentioned subdetectors development we participated on the beam testing of the prototypes and processing of the data from these tests, for both the HEC and TileCal systems. We have been involved in the detector construction, cold testing and commissioning as well. Since the precise knowledge and understanding of the detector behaviour is very important, a detailed Monte-Carlo simulation of the detector is a very important task. Our other obligation has been linked to this effort. The results of our data analysis from the beam testing of the prototypes and our experience with the Monte-Carlo description of the experimental set-up were used as a feedback for Geant4 developers.

The full specification of our commitments to the ATLAS experiment is in the Memorandum of Understanding of ATLAS. Our main commitments to the ATLAS project are:

- final testing of the calibration and readout electronics, confirmation of the electronics functionality according to specifications, and handling to the routine running
- implementation of the electronics calibration procedures within the readout electronics and offline software. These procedures were developed by us, and were tested during the previous test-beams
- contribution to the hadronic energy calibration procedures
- test-beam setups simulations and computing of the first version of calibration parameters
- analysis and preparation for the electronics upgrade.

We also solved some very important technical tasks such as an analysis of the TileCal photomultiplier (PMT) response and carried out the data analysis from the Tilecal test beams. Besides this we are also involved in the ATLAS physics tasks the most of them deals with the top quark physics.

3. HEC beam test calibration

The electronics calibration system was developed for the ATLAS HEC operation and was used in the test-beam testing of various HEC prototypes and Module-0 modules. Besides the main goals of the calibration system, that can be summarized as folows:

- to equalize the gains and to improve possible response nonlinearities of different electronics channels
- to keep the track of timing stability and to provide the corrections in the case of change exceeding predefined level,

the system was used for debugging of the electronics and cables systems.

The detailed studies of the impact of the deteriorations of electronics on the energy jet resolution, one of the main requirements for HEC calorimeter, were carried out [2]. The imperfections of the calorimetric electronics are projected into the constant term of the jet energy resolution. The accuracy of the calibration system is required to be better than 1 % in order not to contribute to the constant term of the jet energy resolution [2].

The system developed by IEP SAS Košice and MPI München was heavily tested against this requirements in the last few years. The system was proved to be satisfactory.

Apart from the calibration system hardware construction and testing, we were involved in the software development and calibration data analysis in all the test-beams of the LAr and TileCal calorimeters on the H6 beam line in CERN.

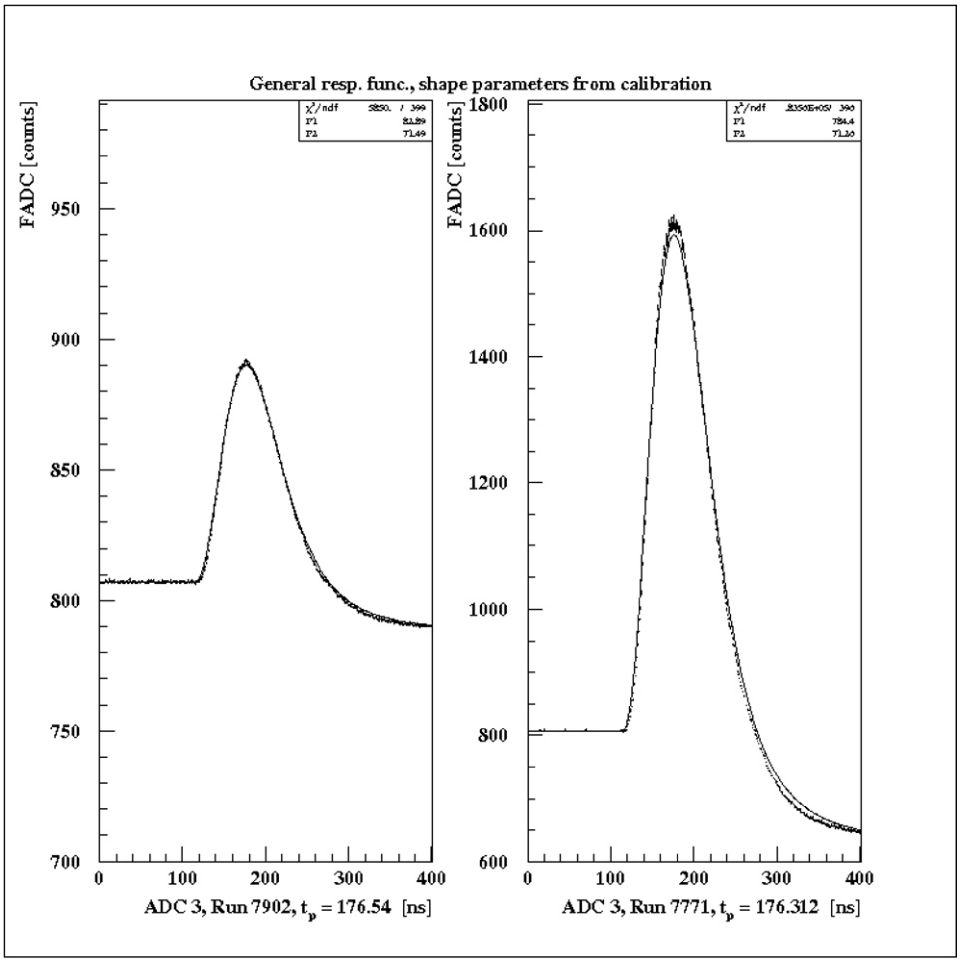

Fig. 1. The electron impulse response fitted with the shape function obtained from calibration.

The optimal filtering method for amplitude reconstruction [3] is assumed to be used in ATLAS, therefore a detailed knowledge of both the amplitude response and the waveform dependence on amplitude is needed.

In connection with this the second aim of hardware calibration is to obtain information on the shape of the waveform from calibration data, because the reliance on particle data can be hampered by limited statistics. The calibration waveform was measured by delaying the calibration pulse with 2.5 ns steps. In order to be able to use the measured calibration waveform for obtaining particle signal waveform, we have chosen to parameterize the impulse response of the read-out system.

The impulse response function $h(t)$ is parametrized [4] as

$$h(t) \quad \sum_{n\ 2}^{N_f} d_n f_n(t)$$

$$f_n(t) \quad \frac{t^{n\ 1}}{(n\ 1)!} \frac{e^{-\frac{t}{0}}}{{}_{0}^{n}} \quad (t) \tag{1}$$

The calibration current $i_C(t) \quad e^{-\frac{t\ t_0}{T_C}} \quad (t \quad t_0)$ is convolved with $f_n(t)$ to produce the calibration waveform:

$$g_C(t) \quad \sum_{n\ 2}^{N_f} d_n F_n(t), \text{where } F_n(t) \quad f_n(t) \star i_C(t) \tag{2}$$

The response to calibration signal is fitted in terms of parameters d_n. We have found that with $N_f \quad 8$ the sufficient accuracy is achieved.

The particle waveform is obtained by using the same basis functions (1) with the fitted parameters d_n, but convoluted with the triangle current $i_p(t) \quad (1 \quad t/T_d)\ (t)$:

$$g_p(t) \quad \sum_{n\ 2}^{N_f} d_n F_n(t) \text{ with } F_n(t) \quad f_n(t) \star i_p(t)$$

Fig. 1 shows the electron data profile in one particular channel, fitted with the shape function with the parameters obtained from the calibration, only the time origin and the amplitude is left free in the fit.

4. The HEC beam tests and MC simulation

The construction characteristics of HEC have been presented in [5]. Originally, the Monte Carlo (MC) description of the HEC test beam setup has been written in the framework of GEANT3 [6]. The results of the GEANT3 simulations and their comparison with the test beam data were presented elsewhere [7].

The simulation package GEANT4 [9] is a new software product, written in C++ program language and fully exploring the object oriented technology, that offers new features. In order not to introduce some "unphysical differences" between the GEANT3 and GEANT4 simulations of our test beam setup, we described the HEC test beam geometry as close as possible in GEANT3 and in GEANT4. In this case, we probably lose some fea-

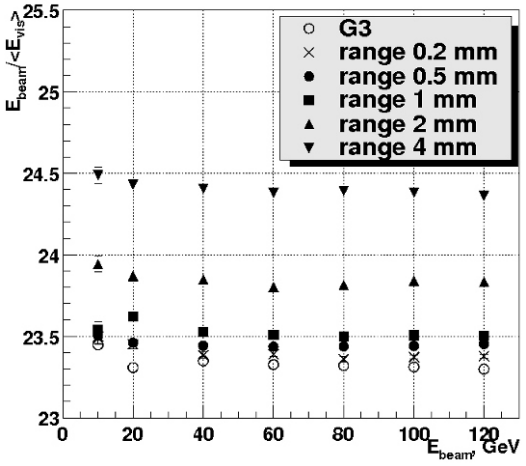

Fig. 2. Inverse sampling ratio for the GEANT3 and GEANT4 simulations.

tures of GEANT4, but our comparison is concentrated on the physical results and not on differences in setup description or even different descriptions of the geometry.

All parts of the test beam setup have been incorporated in the GEANT4 (as in GEANT3): multi-wire proportional chambers (MWPC), scintillation counters and the cryostat.

The output of our simulations consists not only of hits in the sensitive LAr volume, but also in the passive copper absorber plates. This opens a possibility to analyze the simulations in more detail. Also the information from the MWPC has been saved. With this information, we can form some kind of a "trigger". More than one wire hit in a MWPC plane indicates that the beam particle has undergone an inelastic interaction before reaching the cryostat. These events are rejected. The output is saved in a ROOT [10] file in TTree which is similar to Column_Wise_Ntuple (CWN) in the PAW library. Thus, we have practically the same output format in both cases.

As an example we see, in Fig. 2 the energy dependence of the inverse sampling ratio $E_{beam} / E_{visible}$ for the GEANT3 and GEANT4 simulations using various range cuts. As can be seen, the GEANT3 and GEANT4 values are rather close to each other for a range cut of 0.2 mm. With the increasing range cut, the difference between the GEANT4 and GEANT3 increases.

5. GEANT4 physics validation

Due to a big variety of different test-beam results obtained with the ATLAS calorimeter modules, the project for GEANT4 physics validation was started and the Košice group took part also in this activity.

In the first stage, the muon and electron response was studied and compared deliberately with the available test-beam data. For the muons, the main conclusion was that both the GEANT3 and GEANT4 can describe the muon signal spectrum in the HEC quite well.

A Kolmogorov-Smirnoff test yields the same likelihood for both simulated spectra to be identical to the experimental one. The dependence of the tails in the spectrum on the range cut in GEANT4 has been studied as well, clearly indicating a rise in the signal contribution from -electrons when changing the range cut from 4 to 0.2 mm. Then the lower value gives the best description of the experimental data.

On the contrary, the GEANT4 electron signal for electrons in the HEC is systematically about 3 % smaller than the GEANT3 signal, if a 700 m range cut is used. Lowering this cut to 20 m reduces this difference to slightly less than 1 %, see Fig. 3. As can be seen in the same figure, the energy deposited in the absorber is correspondingly larger, so that the total deposited energy is very comparable again. The experimental electron energy resolution is very well reproduced by both the Monte Carlos.

The next round of validations was devoted to the hadron physics, and was published recently [11].

6. TileCal beam test data reconstruction

About 11 % of the 192 TileCal modules were tested by the electron muon and hadron test beams ranging in momentum from 2 to 350 Gev/c. The modules were equipped with the production front-end electronics. All the TileCal calibration systems were used.

The main goals of this testbeam program were:

- to calibrate the energy-to-charge conversion factor using electron beams,
- to explore the response of uniformity of production modules with muon beams,
- to investigate the response of the TileCal modules to hadrons.

The test-beam program used the H8 beam of the CERN SPS North Area. The TileCal modules were placed on a scanning table capable to set position and angle of incoming particle beam. The module 0 (prototype used to check the long time stability of response) is the lowest one, the middle layer is the production barrel model and a pair of production extended barrel modules creates the top layer.

Several geometries were used to calibrate modules:

- beam incident at the center of front face of each front cell at 20 ,
- beam incident at the center of front face of each front cell but at projective angles,
- beam incident at on the side ends of the modules into center of each tile row.

The H8 beam is a mixture of hadrons (typically pions (pions and protons) for negative (positive) beam) muons and electrons. Particles were identified by the TileCal modules response and a pair of Čerenkov counters. The beam position was measured by three wire chambers upstream of the modules. The particles were triggered with three beam scintillators.

The TileCal modules were calibrated with the following systems:

- Cesium Source System. A ^{137}Cs -source was moved through a hole in the scintillating tiles. The goal is to maintain stability of energy calibration at level of 0.5 %.
- Charge Injection System. Each PMT channel is equipped with calibration capacitors which can be charged from a precision voltage source and discharged into input of the electronics. The goal is accuracy of 1 % of calibration of response across all PMTs.
- Laser System. A frequency doubled Nd laser is used to produce light pulses. The pulse is directed to each PMTs through optical fibers. The goal is to calibrate and monitor the PMT response with accuracy better than 0.5 %.

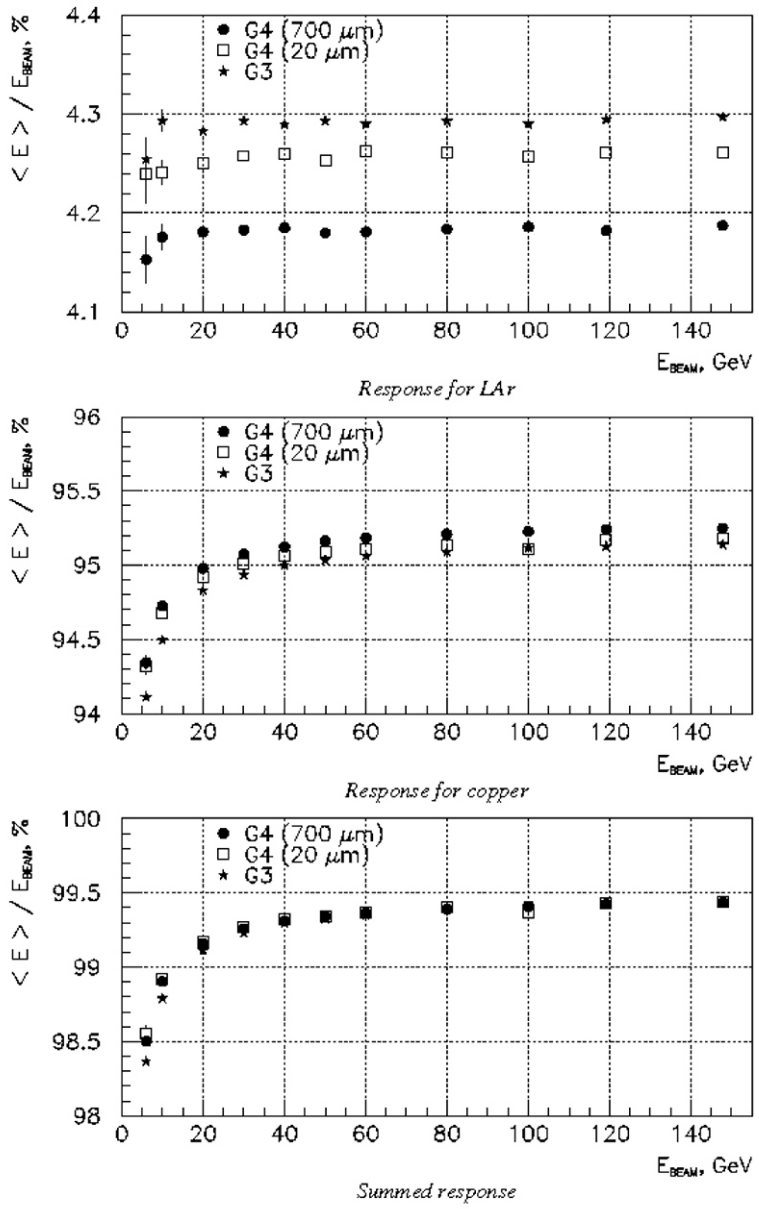

Fig. 3. The energy deposited by electrons in the liquid argon of the HEC calorimeter (left, top), the energy deposited in the absorber (left, center) and the total deposited energy (left, bottom), as a function of the incident beam energy. The plots on the upper right show the relative difference between the GEANT3 (circles) and GEANT4 (triangles) electron signal and experimental data as a function of the cell noise cut level, for 20 and 60 GeV/*c* electrons. The FCal cell signal significance spectrum for 60 GeV/*c* electrons is shown in the bottom right.

A module to module uniformity of 1.9 % was showed with muon beams. The cell to cell variation of electron response is 3 %. The linearity of the modules response to electron beams was found better than 1 %. Measurements of hadron responses indicate a module to module uniformity for hadrons of 1.4 %. The light yield of the calorimeter was 70 pe/GeV exceeding the design goal by 40 %.

7. PMT tests using single photoelectron analysis

Within the task of the Tilecal photomultiplier (PMT) tests a sophisticated PMT response function was suggested for a single photoelectron analysis of the compact metal package photomultiplier spectra. The spectra taken by Hamamatsu R5900 photomultipliers have been analyzed by the presented method. The detailed analysis shows that the method appropriately describes the process of charge multiplication in these photomultipliers and can be used to find their basic internal parameters.

7.1. Photomultiplier Response Function

The output charge spectrum for the case in which n photoelectrons have been created on the photocathode and k on the first dynode, can be expressed as the following convolution [13]:

$$S_{real}(x) \quad \sum_{n,k\ 0} \frac{{}^{n}_{pc} e^{\ pc}}{n!} \frac{{}^{k}_{1} e^{\ 1}}{k!} \quad dx\, S_n^{(1)}(x\ )\ S_k^{(2)}(x\ \ x\ ), \tag{3}$$

where

- $_{pc}$ the light source intensity expressed in number of photoelectrons captured by the PMT dynode system;
- $_1$ the number of photoelectrons created on the first dynode and captured by the following dynode system.

The above shown formula presumes that in the case of two or less photoelectrons collected by the first dynode, the PMT response is not a Gaussian. In this case the response is expressed as a sum of the responses corresponding to different numbers of electrons collected by the second dynode and weighted by the corresponding Poisson factors the number of secondaries created on the dynode by one electron is governed by Poisson statistics.

7.2. Results of analysis

To verify the response function, we took and analyzed a series of faint light (a few photoelectrons) spectra under different conditions. These spectra were analyzed by means of the response function, for the eight dynode R5900 Hamamatsu photomultipliers.

We have shown that the deconvolution method, for analysis of single photoelectron spectra of metal package photomultipliers, works well, at least for the class of the above mentioned PMTs. The example of deconvoluted PMT spectrum is presented in Fig. 4.

The PMT response function employed in this method describes in an adequate way the processes in the metal package photomultiplier and enables to observe also subtle effects

as the photoconversion on the first dynode and/or direct capture of photoelectrons by the second dynode.

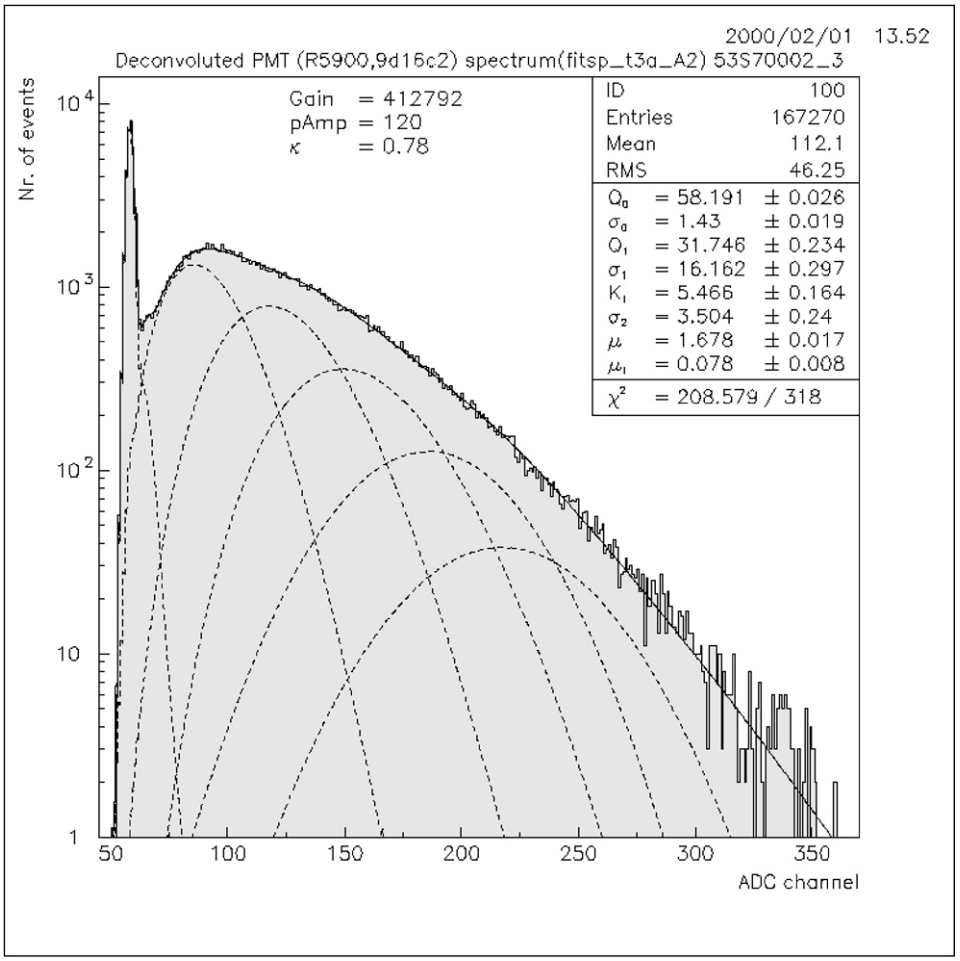

Fig. 4. The deconvoluted LED initiated PMT pulse height spectrum taken at 1000 V by a Hamamatsu R5900 photomultiplier. The first dynode secondary emission coefficient K_1 is treated as an independent parameter.

The method uses only the elementary physical principles and therefore can be easily adapted to other types of photomultipliers.

Our method enables to find important PMT parameters like the position of the charge distribution initiated by one photoelectron (PMT gain) and its standard deviation. On the basis of these parameters, we can calculate the PMT excess factors needed in finding the relation between the mean numbers of photoelectrons and parameters of an experimental spectrum with a high input light signal, and it enables us to calculate the energy-to-signal conversion factor (number of photoelectrons (pe) per GeV) for PMT based calorimeters.

The method can be used as a calibration and monitoring tool for the study of stability in time of a photomultiplier based spectrometric channel.

8. Fast MC simulation of the ATLAS calorimeter

We have developed a new method of the fast Monte Carlo simulation suggested for sampling hadron calorimeters. It is based on the three-dimensional parameterization of the hadronic showers obtained from the ATLAS TILECAL testbeam data and GEANT simulations. A new approach of including the longitudinal fluctuations of hadronic shower is described. The basic idea of the method [8] is in the following. The energy of incident particle is divided into a certain number of energy spots (N). The number N of the spots depends on calorimeter parameters such as resolution and sampling fraction. The energy spots are then distributed over the calorimeter according to the shower profiles. At the same time, each spot has a nonzero probability to be absorbed in active medium and, in such a way, to contribute to calorimeter signal. Simulation of primary interaction of incident particle plays a very important role in this method. A few "principal" output particles are generated from primary interaction and each of the particles is treated separately, i.e. its energy is distributed according to its individual shower profile. The energy of ^{0} is distributed using the electromagnetic shower profile. Such an approach enables us to describe correctly the shower fluctuations. The obtained results of the fast simulation are in good agreement with the TILECAL experimental data as demonstrated in Fig. 5.

Hadron calorimetry is an important part of the high energy physics experiments. Simulation of calorimeter response is an integral part of a calorimeter design and development. It is also inevitable to simulate calorimeter response as a part of full detector response for treating different physics processes to be studied by an experimental setup.

The well known way of the simulation of hadron calorimeter response is to use the GEANT detector simulation package [12]. The GEANT simulations are quite time consuming and it is more convenient in many cases to use the fast simulation methods. In this work we present the fast simulation method, which does not take into account the concrete physical interactions, except of a few most energetic collisions at the beginning of the shower development. The fast Monte Carlo (MC) is based on a three-dimensional parameterization of hadron shower development obtained from the ATLAS TILECAL testbeam data and GEANT simulations.

This fast MC method provides a reliable and fast tool for simulation of hadronic showers in sampling calorimeters. Although it has limits for low energies, it is able to reconstruct correctly the experimental data. The comparison of distributions of energy deposited in different depths along the shower axis proves correctness of the method of longitudinal shower fluctuations.

9. Top Quark physics

One of the tasks solved in frame of the ATLAS physics is determination of the top quark charge. The top quark was discovered in 1995 in the Tevatron experiments (CDF and D0) in Fermilab. Its mass is about 173 GeV/c^2. The charge of the top quark was not measured yet, due to low statistics of the experimental data, though both the D0 and CDF

has already reported on this issue [14, 15]. There are some seculations [16], according to which the quark discovered at Tevatron is not the SM top quark (which should have mass about 270 GeV), but an exotic fourth generation quark with charge - 4/3. The SM top quark is expected to have the charge 2/3.

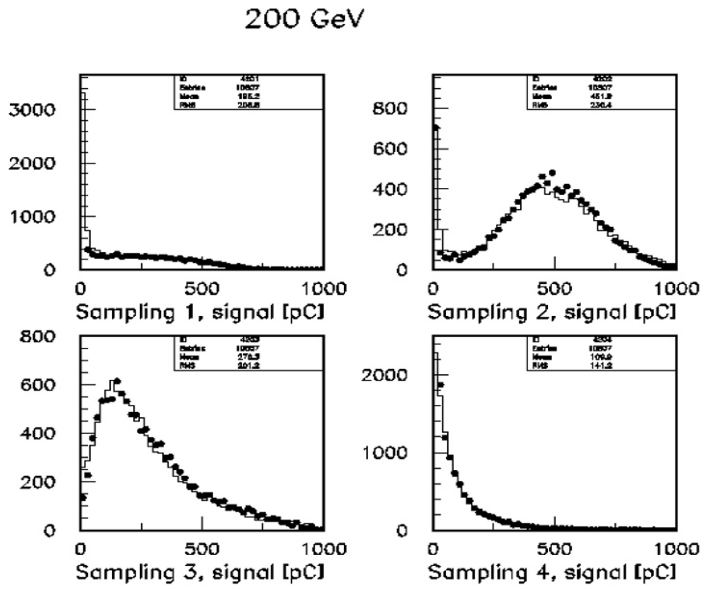

Fig. 5. Comparison of the fast MC and experimental responses for different longitudinal sampling of the TileCal hadronic calorimeter at incident energy 200 GeV, the pion beam was used.

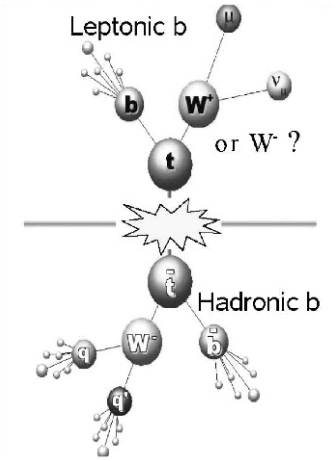

Fig. 6. One of the decay modes of ttbar, so called “lepton + jets channel”. The t(tbar) decays into W and the b. One of the W decays leptonicaly, the other hadronicaly.

The most straightforward way of reconstruction of the top quark charge is to reconstruct it through charges of its decay products. For reconstruction in the lepton + jets channel and the dilepton one (the all jets channel is not good due to huge QCD background), we need to know the charge of the lepton (product of W leptonic decay), to have a method of pairing of the lepton with correct *b*-jet (they should come from the same top quark) and to have a procedure for calculation of the *b*-jet charge.

In the case of the SM top quark, the mean value of the jet charge should have opposite sign to the charge of the associated lepton. In case of exotic, the sign of the jet charge is the same as the charge of the lepton.

For the correct association (pairing) of lepton and *b*-jet a special selection criterion based on lepton-*b*-jet invariant mass ($m(l, b_{jet})$) has been used. The idea is that ($m(l, b_{jet})$) of lepton and *b*-jet coming from the same top quark decay is limited by the top quark mass (m_{top}), while, in case of the lepton and *b*-jet coming from different top quarks, there is no such a restriction, as it is clearly demonstrated by Fig. 7.

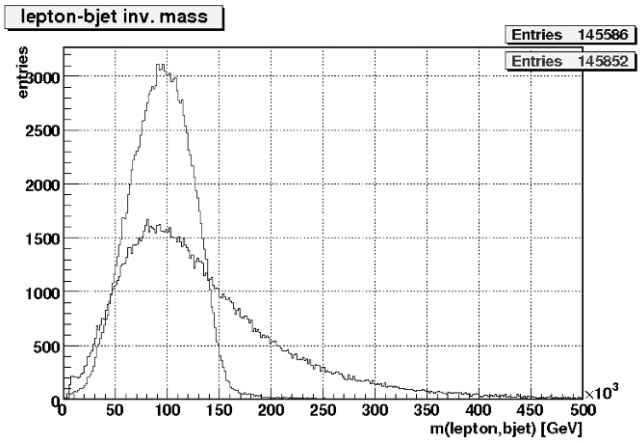

Fig. 7. Lepton bjet invariant mass for the lepton and *b*-jet from the same top quark (red line) and from different top quarks (blue line).

For the jet charge calculation the weighting technique is used the charge of tracks inside *b*-jet cone is weighted according to the formula:

$$q_{bjet} \quad \frac{\sum_i q_i \left| \vec{j} \ \vec{p}_i \right|^k}{\sum_i \left| \vec{j} \ \vec{p}_i \right|^k}, \tag{4}$$

where q_i is the charge of the i^{th} track, j the direction of jet axis, p_i the momentum of the *i*-th track and the optimization coefficient suggested to maximize the diference between the mean *b*-jet charged from *b*- and $\bar{b}$-quarks. The found optimal value of the coeficient is 0.5.

The events selected for the analysis should pass a set of the selection cuts. The transverse momentum p_T of leptons and jets shoud be higher than 25 GeV and 30 GeV, respectively, and the missing transverse energy in the selected events should be higher than

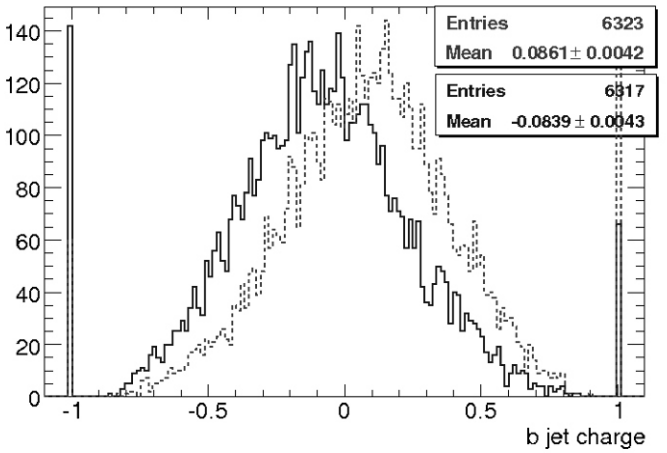

Fig. 8. Charge distribution for *b*-jet associated with positive and negative leptons.

25 GeV (LJ channel) and 40 GeV (DIL channel). Also the tracks for jet charge calculation are required to pass certain quality cuts.

Using the official ATLAS fully simulated events, which take into account all details of the ATLAS detector setup, we managed to reconstruct the *b*-jet charge spectra associated with positive (*b*-jet corresponds to *b*-quark) and negative (corresponds to $\overline{b}$) leptons. As can be seen from Fig. 8, both distributions are neatly distinguishable and thereby the experiment ATLAS has a big potential to distinguish between *b*-jet charge distribution associated with the leptons of different charge (positive or negative). In such a way the ATLAS is capable to decide which hypothesis (SM or alternative exotic one) really occurs, moreover, after a proper calibration of *b*-jet charge, we will be able to find directly the top quark charge.

Acknowledgments

We would like to express our thanks to the Government of the Slovak Republic for their support of the particle physics in Slovakia and our membership at CERN.

We are grateful to Department of Bilateral and Multilateral Cooperation of Ministry of Education of Slovakia for their support.

We would like to express our special thanks to VEGA grant agency for their funding (project 2/0061/08) of some activities. Using these additional financial resources we are particulary able to involve diploma students into our work and to provide some other activities which are not covered by governmental budget.

This work was stimulated and supported by the ATLAS collaboration.

References

[1] *http://en.wikipedia.org/wiki/ATLAS_experiment*.
[2] A. E. Kiryunin: The Influence of Characteristic Parameters of the Electronics Chain of the ATLAS Hadron End-Cap Calorimeter on the Jet Energy Resolution, ATLAS Internal Note CAL-NO-064 (1994).
[3] W. E. Cleland, E. G. Stern: Signal Processing Consideration for Liquid Ionization Calorimeters in a High Rate Environment. NIM A **338** (1994) 467 497.
[4] W. E. Cleland et al.: Dynamic Range Compression in a Liquid-Argon Calorimeter, 6th International Conference on Calorimetry in High-energy Physics: ICCHEP '96 Frascati, Italy, Frascati physics series, **6** (1996) 849 860.
[5] ATLAS Collaboration: Liquid Argon Calorimeter Technical Design Report, CERN/LHCC/96-41 (1996).
[6] A. Kiryunin, D. Salihagić: Monte Carlo for the HEC Prototype: Software and Examples of Analysis, ATLAS-HEC-Note-063 (1998).
[7] A. Minaenko: Test-beam Results for First Serial Modules of ATLAS. Hadronic End-Cap Calorimeter, Proc. of CALOR2000, Annecy, France (2000).
[8] J. Sutiak, S. Tokar, T. Zenis, Y. A. Kulchitsky: New Method of Fast Simulation for a Hadron Calorimeter Response. Particle and Nuclei, Letters **2** [117] (2003) 52 70.
[9] GEANT4 A Simulation Toolkit. NIM A **506** (2003) 250 303.
[10] ROOT An Object Oriented Data Analysis Framework, Proc. AIHEN '96 Workshop, Loussane, NIM A **389** (1997) 81 86.
[11] A. E. Kiryunin, H. Oberlack, D. Salihagic, P. Schacht, P. Strizenec: GEANT4 Physics Evaluation with Testbeam Data of the ATLAS Hadronic End-Cap Calorimeter. NIM **560** (2006) 278 290.
[12] R. Brun, F. Carminati: "GEANT Detector Description and Simulation Tool, W5013", CERN Program Library, CERN, Geneva, Switzerland.
[13] I. Chirikov-Zorin et. al.: NIM A **461** (2001) 587 590.
[14] V. M. Abazov et al. (D0 collaboration): Phys. Rev. Lett. **98** (2007) 041801, preprint FERMILAB-PUB-06/278-E.
[15] A. Abulencia et al. (CDF collaboration): First CDF Measurement of the TopQuark Charge using the Top Decay Products, Public Conference Note, CDFNote 8783, Fermilab, April 13, 2007.
[16] D. Chang, W. F. Chang, E. Ma: Phys. Rev. D **59** (1999) 091503 and Phys. Rev. D **61** (2000) 037301.